

tory. The continuing technical assistance of R. Benesch, the assistance of R. W. Sancton with the video recording system, and that of A. Avery with operation of the CO₂ laser are gratefully acknowledged.

¹M. V. Goldman, *Ann. Phys. (N.Y.)* **38**, 117 (1966); E. A. Jackson, *Phys. Rev.* **153**, 235 (1967).

²C. S. Liu and M. N. Rosenbluth, *Phys. Fluids* **19**, 967 (1976); B. F. Lasinski and A. B. Langdon, *Laser Program Annual Report—1977*, Lawrence Livermore Laboratory Report No. UCRL-50021-77 (unpublished).

³H. C. Pant, K. Eidmann, P. Sachseumaier, and R. Sigel, *Opt. Commun.* **16**, 396 (1976); P. D. Carter, S. M. L. Sim, H. C. Barr, and R. G. Evans, *Phys.*

Rev. Lett. **44**, 1407 (1980).

⁴H. A. Baldis, J. C. Samson, and P. B. Corkum, *Phys. Rev. Lett.* **41**, 1719 (1978).

⁵A. B. Langdon and B. F. Lasinski, in *Methods in Computational Physics*, edited by B. Alder, S. Fernbach, and M. Rotenberg (Academic, New York, 1976), Vol. 16; A. B. Langdon, B. F. Lasinski, and W. L. Kruer, *Phys. Rev. Lett.* **43**, 133 (1979).

⁶N. H. Ebrahim, H. A. Baldis, C. Joshi, and R. Benesch, *Phys. Rev. Lett.* **45**, 1179 (1980).

⁷W. L. Kruer and J. M. Dawson, *Phys. Fluids* **15**, 446 (1972).

⁸H. H. Chen and C. S. Liu, *Phys. Rev. Lett.* **39**, 881 (1977).

⁹H. A. Baldis, C. J. Walsh, and R. Benesch, to be published.

¹⁰J. Sheffield, *Plasma Scattering of Electromagnetic Radiation* (Academic, New York, 1975).

Hard-X-Ray Measurements of 10.6- μm Laser-Irradiated Targets

W. Priedhorsky, D. Lier, R. Day, and D. Gerke

University of California, Los Alamos National Laboratory, Los Alamos, New Mexico 87545

(Received 1 June 1981; revised manuscript received 16 November 1981)

The first measurements of high-energy x-ray emission ($h\nu \sim 30 - 300$ keV) by high-Z microballoon targets irradiated at $5 \times 10^{14} < \phi < 2 \times 10^{16}$ W/cm² by 10.6- μm laser light are reported. An exponential spectrum with a slope $kT_H \sim 250$ keV provides the best fit to spectrometer data at $\phi_i = 10^{16}$ W/cm². The hard-x-ray yield indicates that a substantial fraction, probably between 10% and 100%, of the absorbed laser energy is converted to hot electrons. The slope kT_H is proportional to the fastest ion energy.

PACS numbers: 52.50.Jm, 79.20.Ds

Laser-fusion target performance can be significantly limited by fuel preheat. Energetic electrons created at the laser absorption surface deposit energy in the fuel, preventing efficient compression. The electron distribution may be diagnosed by measurement of high-energy x-ray bremsstrahlung created by electron interaction with the target material. We report the first such measurements of targets irradiated by the 10.6- μm Helios CO₂ laser facility.¹

The slope of the target hard-x-ray continuum was determined by a least-squares fit to signals from a ten-channel array of broadband filter-scintillator channels spanning the region $h\nu \approx 30 - 300$ keV. Five of the channel response functions are shown in Fig. 1. Priedhorsky and Lier describe the instrument, and its calibration, analysis, and background tests in detail.²

A series of gold- or tungsten-coated solacels (hollow nickel microballoons) were irradiated

at a range of focus conditions. The laser energy ranged from 2 to 8 kJ in a 0.75-ns (full width at half maximum) pulse. The targets were 300 and

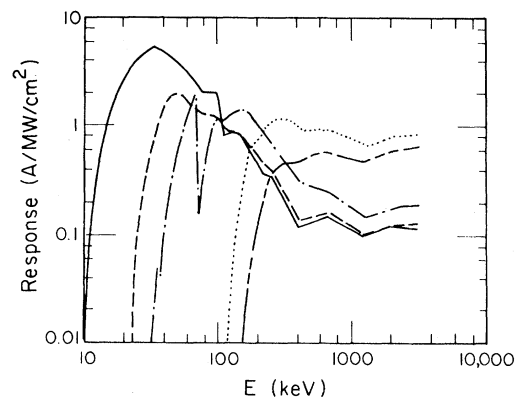


FIG. 1. Five typical spectral response functions from the ten-channel high-energy x-ray spectrometer.

1000 μm in diameter, with 1–2- μm nickel walls coated with 10–15 μm of high- Z material. There is no direct measurement of laser intensity; it is instead estimated from the peak laser power, measured with a pyroelectric detector and normalized by calorimeter data, and from the nominal laser spot size. The laser spot-size diameter containing 50% of the laser energy was determined from earlier encircled energy measurements; shots were taken with 85-, 120-, and 300- μm spot sizes, corresponding to a focus 150, 400, and 1000 μm beyond the irradiated surface. The peak laser intensity averaged over the half-power diameter is $\phi_{1/2} = \frac{1}{2}P/A$, where P is the peak laser power, and A is the half-energy area.

The observed signals could be fitted well by an exponential spectrum,

$$F(h\nu) = A \exp(-h\nu/kT_H), \quad (1)$$

where A is in units of J/keV sr. The kT_H were determined by a least-squares fit. Combining errors in calibration and signal readout, we estimate 1σ errors ranging from 10% to 25% in the detector signals. The smallest errors correspond to the most recent measurements. The spectrometer data were fitted by exponentials with acceptable χ^2 . Given an exponential fit, all kT_H which fit the data with $\chi^2 < \chi_{\text{min}}^2 + 1$ are acceptable at a 1σ level of confidence.³ This confidence level includes random and systematic errors; the relative shot-to-shot error is smaller.

Computer simulations indicate that kT_H is an underestimate of the hot-electron temperature. The calculations assume a Maxwellian electron distribution,

$$dN/dE_e \propto E_e^{(n/2)-1} \exp(-E_e/kT_e). \quad (2)$$

The electron energy is E_e , kT_e is the hot-electron temperature, and n is the dimensionality of the Maxwellian distribution. Theoretical studies of hot-electron generation indicate a Maxwellian electron distribution, with dimensionality n from 1 to 3 depending on the mechanism generating the hot electrons.⁴ Most hot electrons are bound by the target potential, so that they deposit their energy in the vicinity of the target.⁵ In that case, they might produce a "thick-target" bremsstrahlung spectrum, similar to that from an x-ray tube, where the electrons are completely stopped by the target. The classical thick-target bremsstrahlung cross section would yield an approximately exponential x-ray spectrum, with slope kT_e , for an electron distribution as in Eq.

(2). However, preferential loss of energy to fast-ion expansion from the most energetic electrons softens the bremsstrahlung spectrum. Variation of bremsstrahlung cross section and time averaging over the laser pulse also contribute to the discrepancy between kT_H and the peak kT_e . For $kT_e = 100$ –500 keV, the simulations yield approximately exponential x-ray spectra with $kT_H = (0.5$ – $0.8)kT_e$.

The total radiated energy implied by Eq. (1) is $E_x = 4\pi A kT_H$, under the assumption of symmetrical radiation. Because of the flat response of the detectors, E_x can be measured more accurately than the slope kT_H . E_x is calculated from the best-fit spectrum, but for any acceptable kT_H , the implied E_x is within 10% of the best-fit value. E_x is normalized to a fractional x-ray yield $Y = E_x/E_L$, where E_L is the laser energy.

By comparing a Ross-filtered pair of spectrometer channels, we have determined that strong gold K -line emission is not interfering with our estimate of the continuum slope. To a 2σ level of confidence, tungsten $K\alpha$ emission is less than 6.4% of the total integrated hard-x-ray flux.

The best-fit x-ray temperature, kT_H , from the hard-x-ray spectrometer is plotted against $\phi_{1/2}$ in Fig. 2. The data are best fitted by the power law

$$kT_H = 93 \left(\frac{\phi_{1/2}}{10^{15} \text{ W/cm}^2} \right)^{0.42 \pm 0.12} \text{ keV}, \quad (3)$$

for $5 \times 10^{14} < \phi_{1/2} < 2 \times 10^{16} \text{ W/cm}^2$. The uncertainty of the exponent obtains mostly from uncertainty in the laser spot size, and thus $\phi_{1/2}$. We assume that $\phi_{1/2}(150\text{-}\mu\text{m defocus})/\phi_{1/2}(1000\text{-}\mu\text{m defocus})$ is known to within a factor of 2. The scaling of kT_H with energy at constant focal condition is consistent with Eq. (3) (see Fig. 2).

Previous experimental studies have shown

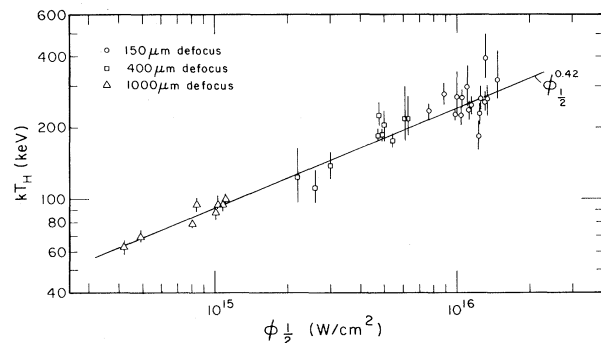


FIG. 2. X-ray continuum slope kT_H as a function of $\phi_{1/2}$ for high- Z shell targets.

much lower x-ray temperatures at 10.6- μm laser intensities which nearly overlap ours.^{6,7} For instance, Enright, Richardson, and Burnett find $kT_H = 10$ keV at $\varphi_{1/2} = 2 \times 10^{14}$ W/cm²,⁷ a value inconsistent with a modest extrapolation of Eq. (3). The earlier experiments involved single-beam illumination of low- Z slabs with a 50–100- μm focal spot, unlike the present high- Z , multiple-beam, large-focal-spot (at low intensity) experiment. Additionally, Enright, Richardson, and Burnett measured the x-ray spectrum from 4 to 25 keV, while the present measurement is weighted to much higher energy. Kephart, Godwin, and McCall showed that the x-ray spectrum at $\varphi_{1/2} \approx 10^{14}$ W/cm² hardens with increasing photon energy⁶; measurement at higher energies thus yields higher temperatures. Our higher kT_H , compared to Refs. 6 and 8, is therefore not surprising. The intensity scaling of Eq. (3) is not inconsistent with previous experimental and theoretical studies, which suggest $kT_H \sim \varphi^{1/3}$.^{7,9}

We observe that the hard-x-ray yield increases with x-ray temperature. Figure 3 shows Y as a function of kT_H . The yield data are bounded by the relationship

$$Y = (1.2^{+0.6}_{-0.4}) \times 10^{-5} kT_H \text{ (keV)}. \quad (4)$$

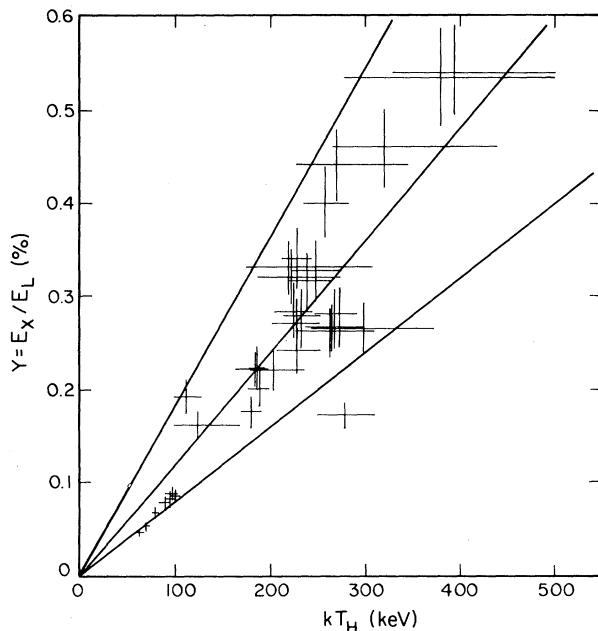


FIG. 3. High-energy x-ray yield Y as a function of kT_H . Y is the fraction of incident laser energy radiated in high-energy x rays. The solid lines show the best fit, and bounds, $Y = (1.2^{+0.6}_{-0.4}) \times 10^{-5} kT_H$ (keV).

The proportionality between Y and kT_H is reminiscent of the classical thick-target bremsstrahlung yield,⁸

$$f_x = 1.1 \times 10^{-6} Z E_e, \quad (5)$$

where f_x is the bremsstrahlung efficiency for monoenergetic electrons of energy E_e (keV) incident on a target of atomic number Z . Keeping in mind that the fast-ion effects which reduce kT_H relative to kT_e also reduce the hard-x-ray yield from a given electron distribution, we would like to derive an estimate of the total energy in hot electrons required to produce the observed spectrum. One calculates, for the spectrum of Eq. (2) and dimensionality $n = 1$ to 3, a classical thick-target yield

$$Y_{tt} = (1.3-2.2) \times 10^{-4} \alpha kT_e \text{ (keV)}, \quad (6)$$

where α is the efficiency of conversion of incident laser energy to fast electrons. Equations (4) and (6) imply

$$\alpha = (0.04-0.14)(Y_{tt}/Y)(kT_H/kT_e). \quad (7)$$

For Y_{tt}/Y and kT_H/kT_e of order unity, Eq. (7) suggests that the inferred electron spectrum is a substantial fraction of the absorbed laser energy (α could be no larger than the laser light fraction absorbed by the target, which is 0.25 for $\varphi \approx 10^{13}-10^{15}$ W/cm²).¹⁰

We observe the correlation between the velocity of the fastest ions emitted by the target and the kT_H from x-ray data, first reported by Tan, McCall, and Williams.¹¹ For planar targets irradiated with a single beam at $10^{12} < \varphi < 10^{14}$ W/cm²,¹¹

$$kT_H = 7.5 \times 10^{-18} v_i^2 \text{ keV}, \quad (8)$$

where v_i is the fastest ion velocity in centimeters per second. Such a proportionality is to be expected for an isothermal expansion into vacuum.¹² At much greater intensity and in a spherical geometry, the same functional dependence holds. The present data can be fitted by

$$kT_H = 19 \times 10^{-18} v_i^2 \text{ keV}, \quad (9)$$

over $5 \times 10^{14} < \varphi_{1/2} < 2 \times 10^{16}$ W/cm².

Measurements of hard-x-ray radiation from 10.6- μm laser-illuminated gold microballoons indicate a very penetrating and intense spectrum, with a best-fit exponential slope ~ 250 keV for $\varphi_i \sim 10^{16}$ W/cm². The hard-x-ray yield implies that a significant fraction of the absorbed laser energy is converted to energetic electrons. The hot-electron population inferred from hard-x-

ray measurements presents a major problem for 10.6- μm laser-fusion target design at high intensities.

We would like to acknowledge helpful comments on the analysis and presentation of these results from D. Wilson, A. Petschek, S. Singer, D. Giovanielli, G. Stradling, and F. Cordova. This work was performed under the auspices of the U. S. Department of Energy.

¹R. L. Carlson *et al.*, IEEE J. Quantum Electron. 17, 1662 (1981).

²W. Priedhorsky and D. Lier, to be published.

³M. Lampton, B. Margon, and S. Bowyer, Astrophys. J. 208, 177 (1976).

⁴K. Estabrook and W. L. Kruer, Phys. Rev. Lett. 40, 42 (1978).

⁵D. V. Giovanelli, J. F. Kephart, and A. H. Williams, J. Appl. Phys. 47, 2907 (1976).

⁶J. F. Kephart, R. P. Godwin, and G. H. McCall, App. Phys. Lett. 25, 108 (1974).

⁷G. D. Enright, M. C. Richardson, and N. H. Burnett, J. Appl. Phys. 50, 3909 (1979).

⁸A. H. Compton and S. K. Allison, *X-Rays in Theory and Experiment* (Van Nostrand, Princeton, 1957).

⁹D. W. Forslund, J. M. Kindel, and K. Lee, Phys. Rev. Lett. 39, 284 (1977).

¹⁰V. M. Cottles, Bull. Am. Phys. Soc. 22, 1090 (1977); D. Giovanielli, private communication; R. Kristal, Bull. Am. Phys. Soc. 25, 1014 (1980).

¹¹T. H. Tan, G. H. McCall, and A. H. Williams, Los Alamos National Laboratory Report No. LA-UR-80-900, 1980 (unpublished).

¹²J. E. Crow, P. L. Auer, and J. E. Allen, J. Plasma Phys. 14, 65 (1975).